Journal of Inorganic Biochemistry 117 (2012) 334–341

Contents lists available at SciVerse ScienceDirect

Journal of Inorganic Biochemistry

journal homepage: www.elsevier.com/locate/jinorgbio

Structural basis behind the interaction of Zn^{2+} with the protein α-synuclein and the Aβ peptide: A comparative analysis

Ariel A. Valiente-Gabioud [a], Valentina Torres-Monserrat [a], Laura Molina-Rubino [a], Andres Binolfi [b], Christian Griesinger [c], Claudio O. Fernández [a,c,*]

[a] Instituto de Biología Molecular y Celular de Rosario, Consejo Nacional de Investigaciones Científicas y Técnicas (IBR-CONICET), Universidad Nacional de Rosario, Suipacha 531, S2002LRK Rosario, Argentina
[b] Department of NMR-assisted Structural Biology, In-cell NMR, Leibniz Institute of Molecular Pharmacology (FMP), Robert-Roessle-Str. 10, 13125 Berlin, Germany
[c] Department of NMR-based Structural Biology, Max Planck Institute for Biophysical Chemistry, Am Fassberg 11, D-37077 Göttingen, Germany

ARTICLE INFO

Article history:
Received 18 April 2012
Received in revised form 22 June 2012
Accepted 22 June 2012
Available online 29 June 2012

Keywords:
Amyloid
Neurodegeneration
Metallobiology
NMR

ABSTRACT

α-Synuclein (AS) aggregation is associated to neurodegeneration in Parkinson's disease (PD). At the same time, alterations in metal ion homeostasis may play a pivotal role in the progression of AS amyloid assembly and the onset of PD. Elucidation of the structural basis directing AS–metal interactions and their effect on AS aggregation constitutes a key step towards understanding the role of metal ions in AS amyloid formation and neurodegeneration. Despite of the reported evidences that link Zn^{2+} with the pathophysiology of PD and the fact that this metal ion was shown to promote AS fibrillation in vitro, neither the structural characterization of the binding sites nor the identification of the amino acids involved in the interaction of Zn^{2+} with the protein AS has been carried out. By using NMR spectroscopy, we have addressed here unknown structural details related to the binding of Zn^{2+} to the protein AS through the design of site-directed and domain truncated mutants of AS. The binding of zinc to the Aβ peptide was also studied and discussed comparatively. Although the results of this study contribute to the understanding of the structural and molecular basis behind the acceleration of AS fibrillation mediated by Zn^{2+}, the low affinity that characterizes the interaction of Zn^{2+} with AS contrasts strongly with the high-affinity features reported for the binding of this metal ion to other target proteins linked to human amylodosis such as Aβ peptide and the Islet Amyloid Polypeptide (IAPP), challenging the biological relevance of zinc interactions in the pathogenesis of PD.

1. Introduction

The misfolding of proteins into a toxic conformation is proposed to be at the molecular foundation of a number of neurodegenerative disorders including Creutzfeldt-Jacob's disease, Alzheimer's (AD) and Parkinson's disease (PD) [1]. One common and defining feature of protein misfolding diseases is the formation and deposition of protein aggregates in various morphologies, including amyloid fibrils [2]. Neurodegeneration in PD is progressive and is characterized by the loss of dopaminergic neurons in the *substantia nigra*, and the presence of amyloid fibrillar aggregates in multiple brain regions containing the protein α-synuclein (AS) [3–6]. α-Synuclein is a highly soluble, intrinsically disordered protein, predominantly expressed in the neurons of the central nervous system and localized at presynaptic terminals in close proximity to synaptic vesicles [7–9]. Evidence that AS amyloidogenesis plays a causative role in the development of PD is furnished by a variety of genetic, neuropathological and biochemical studies [4,5,10–19].

α-Synuclein comprises 140 amino acid residues distributed in three different regions: the N-terminal region, which encompasses residues 1–60, includes the imperfect repeats KTKEGV and is involved in lipid binding [20–22]; the highly hydrophobic self-aggregating sequence known as NAC (non-amyloid-β component, residues 61–95), which initiates fibrillation [23]; and the acidic C-terminal region, rich in Pro, Asp and Glu amino acids, which encompasses residues 96–140 and is essential for blocking rapid AS filament assembly [24–26]. In its monomeric, intrinsically disordered state, the protein is best described as an ensemble of structurally heterogeneous conformations, with no persistent secondary structure and with long-range inter-residue interactions that have been shown to stabilize aggregation-autoinhibited conformations [27–30]. These intramolecular contacts in AS are mainly established between the C-terminus and the NAC regions (hydrophobic interactions), and between the C- and N-terminal regions (electrostatic interactions) [27–29].

Although it remains unclear how AS can initiate neuronal death, it is certain that the amyloid aggregation of AS is essential for the pathological effects associated to PD. Even if amyloid assembly is a complex and multifaceted process, the dominant risk factor associated with PD and other neurodegenerative diseases is increasing age.

* Tel.: +54 341 4448745x731; fax: +54 341 4390465.
E-mail addresses: cfernan@gwdg.de, fernandez@ibr.gov.ar (C.O. Fernández).

0162-0134/$ – see front matter © 2012 Elsevier Inc. All rights reserved.
doi:10.1016/j.jinorgbio.2012.06.011

Several studies indicate that one of the consequences of normal aging is a rise in the levels of metal ions in brain tissue [31,32]. The brain is an organ that concentrates metal ions, and there is now increasing evidence that a perturbation in metal homeostasis may be a key factor in a variety of age-related neurodegenerative diseases. This data support the hypothesis that metal interactions with the target protein in several of these age-dependent degenerative diseases might constitute one of the major factors contributing to their etiology. Accordingly, copper and manganese have been implicated in Creutzfeldt-Jakob's disease [33–36], whereas several studies emphasize the role of copper and zinc as contributors to the neuropathology of AD [34,37–40]. Furthermore, coordination environments for copper complexes in the prion protein, and copper and zinc in the Aβ peptide have been very well characterized by several biophysical and structural studies [35–37,40–61].

The role of metal ions in AS amyloid assembly and neurodegeneration is also becoming a central question in the pathophysiology of PD [62]. Iron deposits were identified in Lewy bodies [63] and elevated copper concentrations were found in the cerebrospinal fluid of PD patients [64]. Analysis of the parkinsonian *substantia nigra* revealed also enhanced levels of zinc in comparison with the control tissues [62,65–68]. Furthermore, epidemiological research indicates that individuals with chronic exposure to copper, manganese, zinc or iron display an increased rate of PD [69]. A comparative analysis between the structural and affinity features of AS complexed to the biologically relevant divalent metal ions copper, iron and manganese demonstrated conclusively a hierarchal effect of AS–metal interactions on AS aggregation kinetics, dictated largely by structural factors corresponding to different protein regions [70,71]. While Fe^{2+} and Mn^{2+} interact at a non-specific, low-affinity binding interface at the C-terminus of AS, Cu^{2+} binds with high affinity at the N-terminal region and it was the most effective metal ion in accelerating AS filament assembly [70,71].

Interestingly, despite of the reported evidences that link Zn^{2+} with the pathophysiology of PD and the fact that this metal ion was shown to promote AS fibrillation in vitro [67,68,72–75], neither the structural characterization of the binding sites nor the identification of the amino acids involved in the interaction of Zn^{2+} with the protein AS have been carried out. Accordingly, in this work we sought to delineate the structural basis behind the interaction of Zn^{2+} with AS, as a first step towards the understanding of the molecular mechanism by which Zn^{2+} accelerates AS filament assembly. The identity of the Zn^{2+} binding ligands and the affinity features of the metal binding sites were elucidated through the design of site-directed and domain-truncated mutants of AS and application of NMR spectroscopy (Fig. 1). These new findings of the bioinorganic chemistry of PD are discussed via a comparative analysis with the Zn^{2+} binding Aβ peptide of AD.

2. Experimental section

2.1. Proteins and reagents

The proteins AS, H50A AS and 1-108 AS were prepared as previously described [25,26]. The H50A mutant was constructed using the Quick-Change site-directed mutagenesis kit (Stratagene) on AS sequence-containing plasmids. The introduced modification was further verified by DNA sequencing. Purified proteins were dialyzed against Buffer A (20 mM MES (2-(N-morpholino)ethanesulfonic acid), 20 mM MOPS (3-(N-morpholino)propanesulfonic acid), 100 mM NaCl, pH range 5.0–7.5), all treated with Chelex (Sigma). $ZnSO_4$ salt of the highest purity available was purchased from Merck. Deuterium oxide was purchased from Sigma. Non-labeled and ^{15}N isotopically enriched Aβ(1–40) samples were purchased from EZBiolab and Alexotech, respectively. Peptides were dissolved in 10 mM NaOH solutions and stored at −80 °C. Prior to performing the NMR experiments, Aβ samples were dissolved in Buffer B (20 mM TRIS, pH 7.5) and centrifuged at 20,000 *g* to eliminate potentially pre-formed aggregates [76].

2.2. NMR spectroscopy

NMR spectra were acquired on a Bruker Avance II 600 MHz spectrometer using a triple-resonance probe equipped with z-axis self-shielded gradient coils. Heteronuclear Single Quantum Coherence (HSQC) spectra were registered at 15 °C on 100 μM ^{15}N-labeled AS samples dissolved in Buffer A or at 5 °C on 100 μM ^{15}N-labeled Aβ samples dissolved in Buffer B. 1D ^1H NMR experiments were acquired at 15 °C on 100 μM unlabeled AS samples prepared in buffer A and dissolved in D_2O, or on 50 μM unlabeled Aβ samples dissolved in deuterated Buffer B. Aggregation of AS and Aβ did not occur under these low temperature conditions and absence of stirring.

Residual dipolar couplings (RDCs) were measured on ^{15}N-AS samples aligned in 5% (w/v) n-octyl-penta(ethylene glycol)/octanol (C8E5) [77]. Formation of the anisotropic, dilute liquid crystalline phase was monitored by the splitting of the deuterium signal and ranged on 20 ± 2 Hz. One-bond N–H residual dipolar couplings (D_{NH}) were acquired using the 2D inphase–antiphase (IPAP)-HSQC sequence under both isotropic and anisotropic conditions [78].

For the mapping experiments, ^1H–^{15}N HSQC amide cross-peaks affected during metal titration were identified by comparing their chemical shift values with those of the same cross-peaks in the data set of samples lacking the metal ion. Differences in the mean weighted chemical shift (MWΔCS) values for ^1H and ^{15}N were calculated as $[(\Delta\delta^1H)^2+(\Delta\delta^{15}N/10)^2]^{1/2}$ [79]. Intensity profiles (I/I_0) were obtained by comparing the intensities of ^1H–^{15}N HSQC amide cross-peaks registered in the presence (I) and absence (I_0) of the

Fig. 1. Primary sequences of Aβ (1–40) peptide (upper panel) and AS (lower panel). Residues shaded in black represent the main Zn^{2+} anchoring moieties in both biological systems. In the upper panel, underlined residues locate the regions experiencing severe broadening upon Zn^{2+} binding (see text for details). In the lower panel, the N-terminal, NAC and C-terminal regions of AS are indicated. Dotted lines and the grey box locate clusters of negative charges and regions with residual structure at the C-terminus, respectively.

metal ion [71,80–83]. The I/I_0 ratios of non-overlapping cross-peaks were plotted as a function of the protein sequence to obtain the intensity profiles.

The affinity features of Zn^{2+} binding to the protein AS were determined from 2D ^1H–^{15}N HSQC and 1D ^1H NMR experiments on 100 μM protein samples recorded at increasing concentrations of the metal ion. Depending on the protein variant used in the experiments, changes in chemical shift values of the selected amide resonances were fitted to a model incorporating one Zn^{2+} ion per molecule (with an apparent dissociation constant K_{d1}) or were fitted simultaneously to a model incorporating complexes of Zn^{2+} in two classes of independent, non-interactive binding sites per protein molecule (with apparent dissociation constants K_{d1} and K_{d2}). The program DynaFit was used in the affinity analysis [84].

Acquisition, processing and visualization of the NMR spectra were performed by using TOPSPIN 2.0 (Bruker) and Sparky (Goddard and Kelner, UCSF).

3. Results

3.1. NMR mapping of the AS–Zn^{2+} complexes

The details of Zn^{2+} binding to the protein AS were explored at a single-residue resolution level by using NMR spectroscopy. ^1H–^{15}N heteronuclear single quantum correlation NMR spectra (HSQC) contain one cross-peak for each amide group in the molecule (except those involving prolines) and thus provide multiple probes for locating Zn^{+2}-binding sites. The ^1H–^{15}N HSQC spectrum of 100 μM of uniformly ^{15}N-labeled AS recorded at 15 °C is shown in Fig. 2A. The resonances were well resolved and sharp, with a limited dispersion of chemical shifts, reflecting the unfolded nature and the high degree of backbone mobility of the protein.

Upon titration of ^{15}N-enriched AS with increasing concentrations of Zn^{2+} the ^1H–^{15}N HSQC spectra retained the excellent resolution of the uncomplexed protein but demonstrated significant backbone chemical shift changes in a discrete number of residues located at the N- and C-terminal regions of the protein (Fig. 2A). The strongest effects at 100 μM Zn^{2+} were centered on the amide group of Asp121 in the C-terminal region, whereas at higher levels of the added metal ion (~300 μM) a clear effect became evident at the N-terminal region centered on the amide group of His50 (Fig. 2A). The changes at the C-terminus were further pronounced and generalized at higher levels of Zn^{2+} (~500 μM), likely reflecting the transient population of secondary sites at the C-terminus (Fig. 2A). No broadened or new resonances appeared (Fig. 2B), discarding the occurrence of metal-induced exchange broadening processes, such as slow or intermediate chemical exchange between free and metal-bound species or the formation of intermolecular metal-bridged complexes. Instead, the observed displacements of the chemical shifts at the N- and C-terminus regions were continuous, monotonic functions of the metal ion concentration, indicative of a system undergoing fast exchange on the NMR chemical shift timescale. Interestingly, with the exception of residues located in the vicinity of His50, the amide resonances of residues assigned to the N-terminal or NAC regions remained unaltered at higher Zn^{2+} concentrations. All NMR spectral changes induced by Zn^{2+} were abolished upon EDTA addition, confirming the reversibility of Zn^{2+} binding (data not shown).

The role of His50 and Asp121 as main anchoring residues for Zn^{2+} binding to AS is clearly evidenced by the mean weighted chemical shift profiles (MWΔCS) shown in Fig. 3A. However, the observed behavior may be consistent with binding of Zn^{2+} ions to (i) separate, non-interacting sites located at the N- and C-terminus of AS or (ii) a single metal binding interface formed by the structural reorganization of the affected regions. Therefore, to investigate the role played by the affected regions and the influence of transient AS long-range interactions on the binding event, we performed titration experiments with Zn^{2+} ions on protein variants containing point mutations or domain-truncations designed to eliminate binding to one of the potential Zn^{2+} sites (Fig. 1). In order to determine the implications of His replacement on the Zn^{2+} binding features to the N-terminal region, the MWΔCS profile of the H50A AS mutant was measured (Fig. 3B). Comparison of this profile to that of the wild-type species revealed that the changes induced by Zn^{2+} in the region containing the His residue were the only ones abolished upon mutation of this site, confirming that His is the anchoring residue for Zn^{2+} binding to the N-terminal region of AS and, demonstrating that the identified Zn^{2+} sites at the N- and C-terminal regions of the protein constitute independent, non-interacting motifs. A similar behavior was observed upon deletion of the 109–140 region of AS, as revealed by the presence of the Zn^{2+} binding component centered on His50 in the MWΔCS profile measured for the C-terminal truncated variant 1-108 AS (Fig. 3C). Further support to these findings comes from the measurements of the chemical shifts perturbations induced by Zn^{2+} ions on the resonances of Hε and Hδ protons in the imidazol ring of His50, as monitored by 1D ^1H NMR experiments registered on the 1-108 AS variant (Fig. 4A–B). Altogether, these data demonstrate conclusively that the transient long range interactions in AS do not influence the binding preferences of Zn^{2+} at each site.

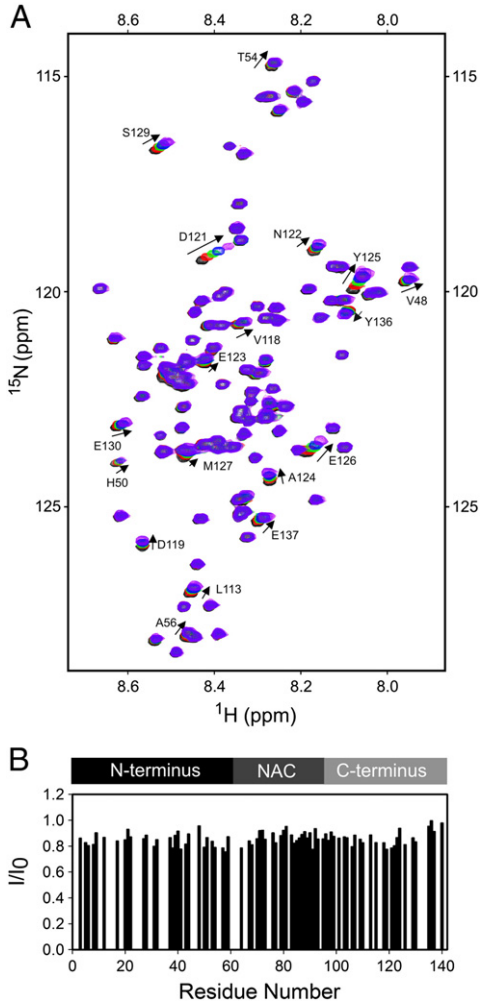

Fig. 2. NMR analysis of Zn^{2+} binding to AS. (A) Overlaid ^1H–^{15}N HSQC spectra of AS (100 μM) in the absence (black) and presence of 100 μM (red), 300 μM (green), 500 μM (blue) and 1000 μM Zn^{2+} (purple). Amino acid residues affected by the interaction with Zn^{2+} ions are identified. (B) I/I_0 profiles of the ^1H–^{15}N HSQC NMR signals of 100 μM AS in the presence of 500 μM Zn^{2+}.

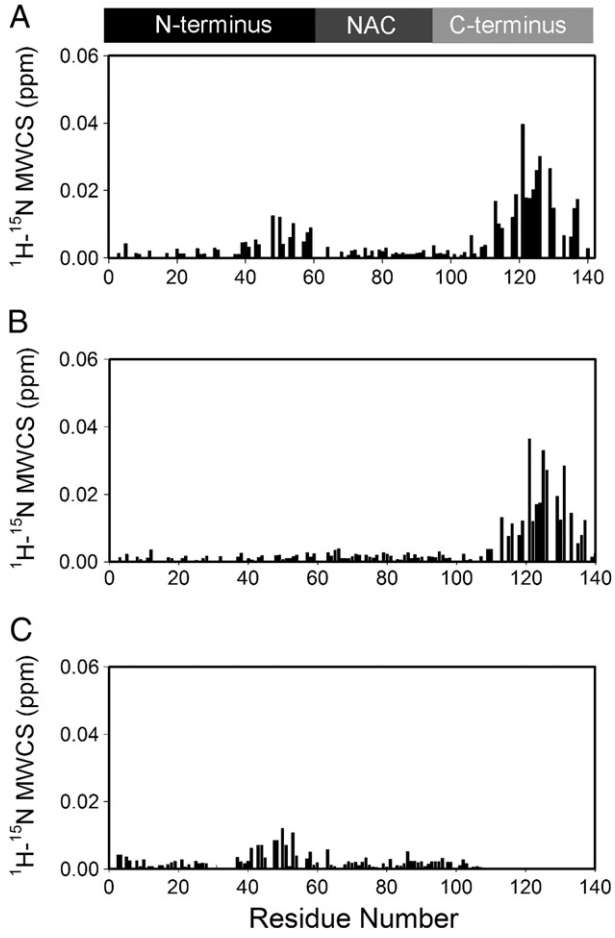

Fig. 3. Differences in the mean weighted chemical shift displacements (MW ^{1}H–^{15}NΔCS) between free and Zn^{2+} complexed AS (A), H50A AS (B) and 1-108 AS (C) at a molar ratio of 5:1.

3.2. Zn^{2+} binding to AS is a low affinity process

To assess the affinity features of the AS–Zn^{2+} interaction, the dissociation constants of the AS–Zn^{2+} complexes were determined by NMR spectroscopy. Upon addition of Zn^{2+} to AS samples, the residues exhibiting the largest displacements in the amide resonances at the C-terminus were Asp121 and Asn122, while the amide resonances of Val48 and His50 were the most affected signals at the N-terminus. All these cross-peaks were well resolved over the entire Zn^{2+} titration experiment and thus well suited for the calculation of dissociation constants (K_d's). By considering a model incorporating complexes of Zn^{2+} in two classes of independent, non-interactive binding sites, the NMR-derived K_d's for the AS–Zn^{2+} complexes involving His50 and Asp121 were 1.3 ± 0.3 and 1.1 ± 0.2 mM, respectively (Fig. 5A). As expected, the data measured for H50A AS and 1-108 AS variants fit to a model that assumed binding of 1 equivalent of Zn^{2+} per molecule (Fig. 5B–D). From these experiments, we also estimated K_d values in the mM range for the H50A AS–Zn^{2+} (1.1 ± 0.3 mM) and 1-108 AS–Zn^{2+} (1.2 ± 0.2 mM) complexes. These results demonstrate conclusively the existence of independent, non-interacting sites at the N- and C-terminal regions of AS, with mM affinities for the metal ion. Overall, the evidences showed here indicate that the interaction of Zn^{2+} with AS is a very low affinity process. Interestingly, physiological levels of Zn^{2+} in mammalian brains are in the 10–20 nM range [85], whereas increments up to 50% of these levels were reported in the *substantia nigra* of PD patients [62,65,66]. Comparatively, Zn^{2+} levels in the mM range have been reported in amyloid plaques of AD patients [86]. Thus, the low affinity features characterizing the binding of Zn^{2+} to AS challenge the biological relevance of AS–Zn^{2+} interactions in the pathogenesis of PD.

3.3. Structural determinants of Zn^{2+} binding to AS

As previously reported, residual dipolar couplings (RDC) constitute an excellent tool to characterize the slow-dynamics of AS in its monomeric state [27,87]. The RDC profile of AS is characterized by predominantly positive couplings that become exceptionally large for residues 115–119 and 125–129 in the C-terminus, indicative of a higher degree of restricted motions in that region (Fig. 6A). Interestingly, the residues being affected primarily in the C-terminus by the lower concentrations of added zinc were Asp121, Asn122 and Glu123, which are contained in the linker sequence showing couplings close to zero and connecting the two major peaks of the RDC profile (115–119 and 125–129) (Fig. 6B). The strong correlation between the location of the primary Zn^{2+} binding site in the C-terminus and the dynamic and structural properties inherent to that region suggests that the presence of a specific spatial organization about residues 121–123 might result in a particular orientation of the coordination moieties favoring metal binding to this region [71]. Indeed, despite the presence of a cluster of negatively charged residues around Asp135, comprising Glu130, Glu131, Glu137, and Glu139, a noticeable difference was observed in the metal binding capabilities of the regions centered on Asp121 and Asp135. Consistent with the binding of other divalent metal ions to the C-terminal region, we can conclude that the binding of Zn^{2+} ions to the C-terminus of AS is not driven exclusively by electrostatic interactions but mostly modulated by the intrinsic conformation of that region [71]. Interestingly, no substantial changes were observed in the RDC profile of AS in the presence of mM levels of Zn^{2+}, revealing that the dynamic and structural features of the protein are not severely affected upon metal-complex formation (data not shown).

The results presented in this section provided compelling evidence for a common low-affinity metal binding interface at the C-terminus, whose structural and dynamic properties determine the preferences of binding of divalent metal ions to that region. On the other hand, the low-affinity binding of Zn^{2+} to the N-terminal region is related to the presence of a single histidine located in an unstructured region of the

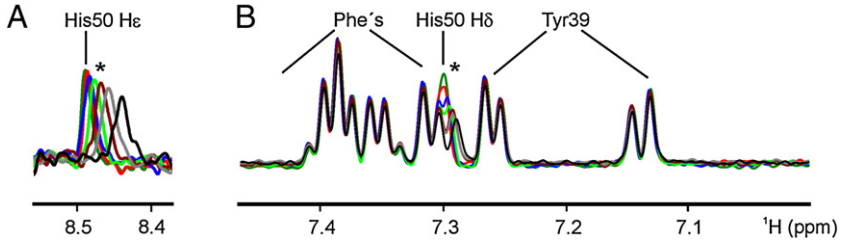

Fig. 4. 1D ^{1}H NMR of aromatic side chains of 1-108 AS in the presence of Zn^{2+} ions. Spectra were registered at 15 °C in D_2O on samples containing 100 μM 1-108 AS in the absence (dark green) and presence of 50 μM (red), 150 μM (blue), 250 μM (green), 350 μM (dark red), 500 μM (grey) and 1000 μM (black) Zn^{2+}. Panels (A) and (B) show the region of the spectra encompassing the Hε imidazole resonance of His50 and the aromatic side chains of 1-108 AS, respectively. The positions of the Hε and Hδ imidazolic protons of His50 are indicated with an asterisk.

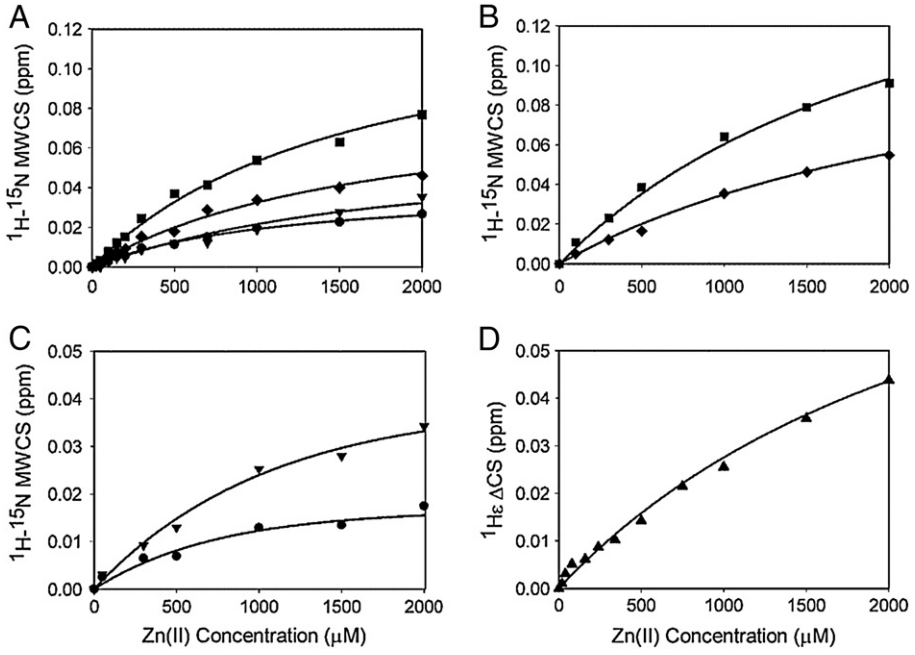

Fig. 5. Affinity features of Zn^{2+} binding to AS. Panels show the binding curves of Zn^{2+} to AS (A) and its variants H50A AS (B) and 1-108 AS (C, D). Formation of the AS–metal complexes were monitored in A–C by changes in the MW ^{1}H–^{15}NΔCS values of amide groups of Asp121 (squares), Asn122 (diamonds), Val48 (circles) and His50 (triangles down). Changes in the ^{1}H ΔCS values of the imidazolic proton Hε of His50 were used in D. Curves represent the fit to the models described in the text, by using the program DynaFit.

protein, being mostly determined by the efficient role played by imidazole side-chains as metal-chelating anchoring groups [88,89].

3.4. Structural features of Aβ-Zn^{2+} complexes

The structural features of Zn^{2+} binding to Aβ peptide were also explored by measuring the ^{1}H–^{15}N HSQC spectra of Aβ(1–40) peptide (Aβ40) in the absence and presence of increasing concentrations of Zn^{2+} (Fig. 7). The tendency of the Aβ40 peptide to aggregate is higher than AS and, thus, all the measurements were conducted at the low temperature of 5 °C and peptide concentration of 100 μM, where the sample remains stable.

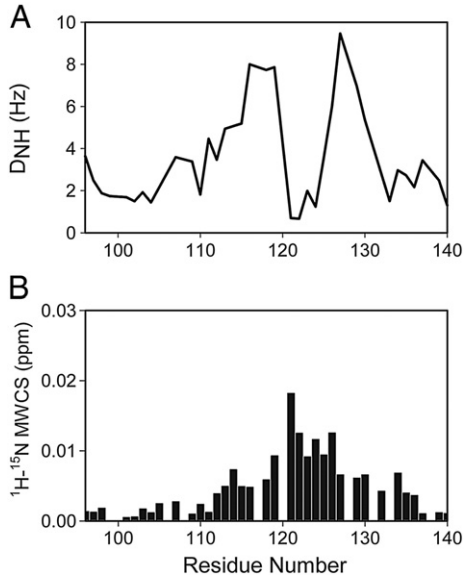

Fig. 6. RDC and MW ^{1}H–^{15}NΔCS profiles of backbone amide groups in the C-terminal region of AS (residues 96–140). (A) Expansion of the ^{1}H–^{15}N RDC profile of 100 μM AS aligned in C8E5 medium at 15 °C. (B) MW ^{1}H–^{15}NΔCS profile of 100 μM AS in buffer A at 15 °C upon addition of 100 μM Zn^{2+}.

As previously reported, the spectral changes observed upon Zn^{2+} addition were centered on residues His6, His13 and His14, clearly indicating the involvement of the imidazole ring of these residues as metal coordinating moieties (Fig. 7). In contrast to the binding behavior observed for the AS–Zn^{2+} complexes, the affected Aβ40 resonances were severely broadened by the addition of substoichiometric concentrations of zinc (0.2–0.5 equivalents) (Fig. 7A). Further addition of Zn^{2+} caused the Glu3, Phe4, Arg5, Asp7, Glu11, Val12, His13, Gln15, Lys16 signals to be broadened beyond detection (Fig. 7B), indicative of a system undergoing intermediate exchange on the NMR chemical shift timescale.

To gain further insights into the structural determinants of the exchange broadening process monitored by backbone amide resonances (amide cross-peaks of His6 and His14 are not detected due to severe signal overlapping), we performed NMR experiments aimed at detecting the resonances of aromatic side chains. Changes in the ^{1}H NMR spectra of the side chains of a protein are sensitive probes for detecting metal binding and defining the binding interface. The ^{1}H NMR spectrum of Aβ40 in D_2O shows well-resolved clusters of resonances in the 6.5–8.0 ppm range, comprising the side chains of different aromatic residues: Phe4, His6, Tyr10, His13, His14, Phe19 and Phe20 (Fig. 8A). The distribution of these residues throughout the Aβ sequence provides excellent probes for exploring the binding features of metal ions to Aβ40.

As observed in Fig. 8B–C, addition of 0.2–0.4 equivalents of Zn^{2+} caused significant line broadening effects on the resonances of His6, Tyr10, His13 and His14. Further addition of Zn^{2+} (≥0.5 equivalents) caused the His6,13,14 and Tyr10 signals to be broadened beyond detection (Fig. 8D), once more indicative of a system undergoing intermediate exchange on the NMR chemical shift timescale. Altogether, the 1D and 2D NMR titration experiments showed that the degree of broadening induced by Zn^{2+} ions on the aromatic side chains of Aβ40 decrease in the order His6,13,14 > Phe4,Tyr10 ≫ Phe19,Phe20, confirming that histidines at positions 6, 13 and 14 constitute the main anchoring residues for Zn^{2+} binding to Aβ40.

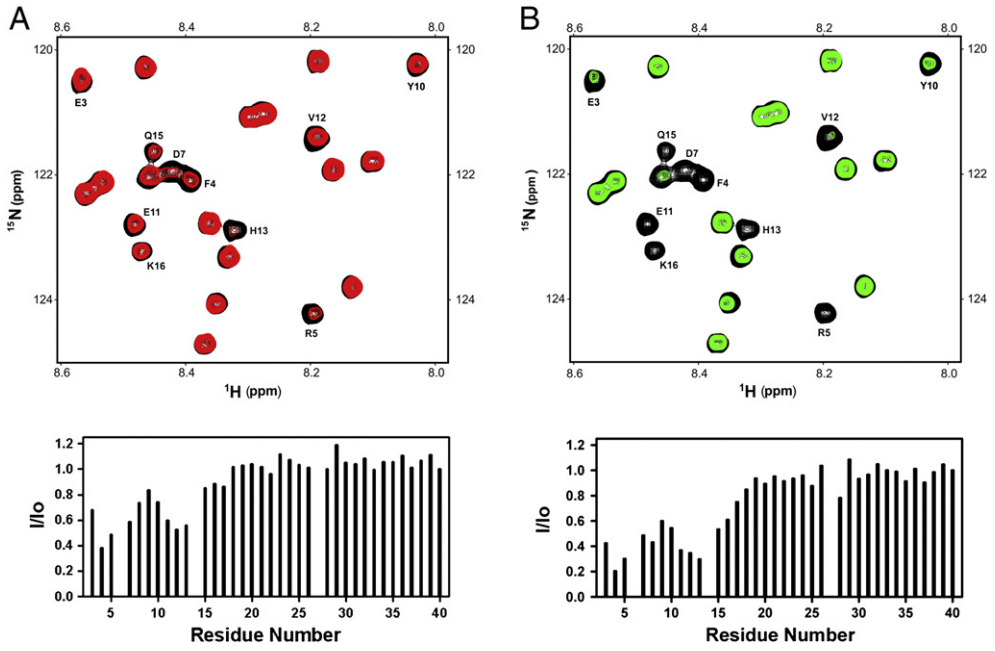

Fig. 7. NMR analysis of Zn^{2+} binding to Aβ. Overlaid ^{1}H–^{15}N HSQC spectra of Aβ (100 μM) in the absence (black) and presence of 20 μM (red — or gray in the print version) (A) and 70 μM Zn^{2+} (green — or gray in the print version) (B). The I/I_0 intensity profiles of the backbone amide resonances of Aβ in the presence of Zn^{2+} are reproduced below each overlaid ^{1}H–^{15}N HSQC spectra. Intensities were normalized using the intensity of the amide cross-peak of Val40.

4. Discussion

Metal ions, especially copper, zinc and iron are considered as risk factors for AD and PD based on clinical and epidemiological studies [31,32]. The simplest mechanism proposed involves a direct effect of the metal ions on the aggregation of the target proteins linked to these diseases. The effects reported for Zn^{2+} ions on AS fibrillation revealed that metal concentrations in the mM range, far greater than those normally occurring in tissues, are necessary to accelerate the amyloid aggregation of the protein [67,68,72–75], which argue against the physiological relevance that these effects might have on the etiology of the disease. Furthermore, no structural characterization of the Zn^{2+} binding sites, or the identification of the amino acids involved in the metal–AS interactions has been reported to date. The lack of structural and affinity data supporting the reported effects of Zn^{2+} on AS aggregation in vitro was the driving force that prompted us to address these unresolved details related to the binding of Zn^{2+} ions to AS. In this work we sought to characterize structurally the interaction of Zn^{2+} with AS by mapping their binding sites and analyzing the affinity features for this interaction through a comparative study with the Aβ peptide of AD.

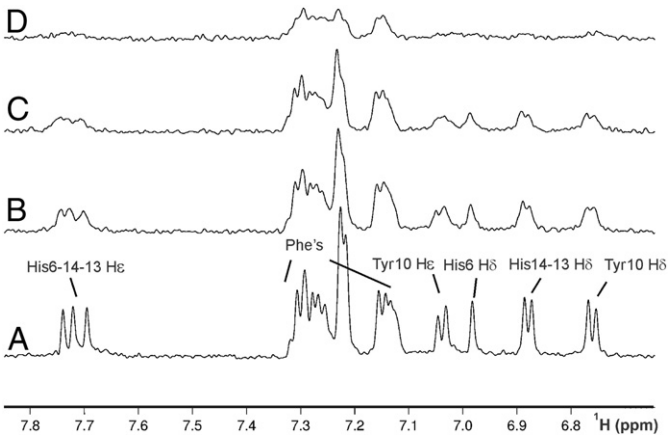

Fig. 8. NMR analysis of Zn^{2+} binding to aromatic side chains of Aβ. 1D ^{1}H NMR spectra of Aβ (50 μM) in the absence (A) and presence of 10 μM (B), 20 μM (C) and 50 μM of Zn^{2+} (D).

The NMR analysis of the AS–Zn^{2+} complexes indicated that an interface with multiple binding sites for Zn^{2+} exists in the region comprising residues 110–140 at the C-terminal domain of AS. At concentrations of Zn^{2+} in the 50–100 μM range, the metal interaction was highly localized around residues Asp121, Asn122 and Glu123, the spectral features of the former being the most affected. The structural picture of this binding event, characterized by a dissociation constant in the mM range, resulted to be very similar to that determined for the AS–metal complexes involving the Cu^{2+}, Fe^{2+}, Mn^{2+}, Co^{2+} and Ni^{2+} ions [71]. Altogether, the data prove conclusively that the binding of Zn^{2+} to the C-terminus of AS takes place primarily in a well-defined region, likely involving Asp121 as the main anchoring residue, and that the protein AS binds metals to the C-terminus with very low selectivity.

Interestingly, as observed for Cu^{2+} ions, a Zn^{2+} binding site was also identified in the unstructured N-terminal region around the sole His50 residue. Our study demonstrated conclusively that the imidazol ring of the histidine residue is the anchoring group for zinc binding to the N-terminal region of AS. However, the affinity features reported for the AS–metal complexes at this site varies from 35 μM in the case of Cu^{2+} ions [81] to around 1 mM for Zn^{2+} ions. Contrasting with the lack of selectivity that characterizes the binding of metal ions to the C-terminus, a hierarchy seems to exist for AS–metal interactions at the His50 site, likely determined by the nature of the metal ion involved and its coordination geometry preferences. Indeed, Cu^{2+} is known to promote ionization of amide groups of peptides if a histidine residue is available as a primary binding site, forming preferentially an intramolecular His(N_π)/amide(N^-)–Cu^{2+} chelation environment [90], as has been reported recently for the AS–Cu^{2+} complex formed at the His site [91]. In contrast, zinc prefers to bind four to six ligands, promoting intermolecular His(N)–Zn^{2+}–His(N) metal-bridged complexes [61,92,93]. However, the NMR structural characterization and the dissociation constant reported here for the His50–Zn^{2+} complex argue against the formation of an intermolecular zinc-bridged complex. Indeed, as will be

discussed in the next paragraph, our results support the existence of a metal complex formed by the individual coordination of the imidazol ring of the sole His50 to Zn^{2+}.

At this juncture a tighter link with other Zn^{2+} binding amyloid proteins can be sought, based on these new insights into the structural basis of zinc interactions with AS. Unlike the Aβ peptide, that binds zinc tightly in a coordination environment that involves participation of histidines located at positions 6, 13 and 14, the protein AS contains only one histidine residue (His50) that is able to coordinate Zn^{2+} weakly at the N-terminal region of the protein. Multiple Zn^{2+} binding sites involving Asp and Glu residues exist also in the C-terminal region of AS, that show affinity features similar to that of the His50–Zn^{2+} complex at the N-terminus. Interestingly, the Zn^{2+} binding region of Aβ40 contains, in addition to histidines 6, 13 and 14, other potentially metal ion coordinating amino acids such as Asp (positions 1, 7 and 23) and Glu (positions 3, 11 and 22); however, opposite to our findings in AS, the relative Zn^{2+} binding efficiencies of Asp and Glu residues in Aβ are insignificant as compared to that of histidines [94].

Individually, the imidazole of a single histidine has a dissociation constant for zinc in the low millimolar range [95,96], which is similar to that revealed here for the His50–Zn^{2+} complex but that is significantly higher than the low micromolar binding (K_d ~ 1–15 μM) reported by several studies for the Aβ–Zn^{2+} complex [40,58,59,97,98]. Thus, the presence of a zinc coordinating motif formed by histidine residues located at different locations of the Aβ sequence, compared with the sole His50 in AS, seems to be the key difference that influences the structural and affinity features for Zn^{2+} in these proteins. Indeed, a minimum of three histidines is also required to obtain the low micromolar affinity complex formed between Zn^{2+} and the islet amyloid polypeptide (IAPP), related to type II diabetes [92]. The IAPP molecule contains only one residue (His18) that binds zinc tightly (K_d ~ 1 μM), resulting from the coordination of six IAPP molecules with a single zinc [92,99]. Intermolecular binding modes are also promoted by Zn^{2+} binding to Aβ, giving rise to a network of Aβ peptides that are cross-linked by a Zn^{2+} bridge binding histidines belonging to adjacent peptides [40,100,101]. Whereas the relatively unstructured nature of IAPP and Aβ peptides may facilitate additional metal-bound ligands [102,103], the existence of transient long-range interactions and the partial lack of conformational flexibility of AS might be the main structural factors disfavoring the formation of zinc-bridged, intermolecular complexes.

In addition to demonstrating the existence of important structural differences between the AS–Zn^{2+} and Aβ–Zn^{2+} coordination modes, our study may contribute to understand the molecular origin of the impact that these interactions exert on the amyloid fibril formation of these proteins. Indeed, whereas the formation of high-affinity, intermolecular Zn^{2+} complexes in Aβ prevents amyloid fibril formation, likely by stabilizing non-fibrillar species or inducing extensive amyloid polymorphism [101,104,105], the low-affinity binding of Zn^{2+} ions to AS results in the formation of intramolecular AS–Zn^{2+} complexes and acceleration of the amyloid fibril formation of the protein. Overall, a coordination site formed mostly by carboxylate moieties or a single imidazol ring is in agreement with the modest affinity constants observed for Zn^{2+} binding to AS, and thus the high levels of this metal ion required to induce the aggregation of AS [75]. Regarding the molecular mechanism behind Zn^{2+} induced acceleration of AS fibrillation, it was proposed to be mediated exclusively by the binding of the metal ion to the negatively charged carboxylates in the C-terminal region, leading to masking of the electrostatic repulsion and the collapse to a partially-folded conformation [106,107]. As might be noted, this hypothesis does not consider His50 as a residue playing an active role in the Zn^{2+}-mediated acceleration of AS fibrillation. Overall, our previous structural studies in the field of the bioinorganic chemistry of PD and the NMR evidences shown here argue against the presence of significant conformational changes in AS induced by the interaction with Zn^{2+}, either the induction of a partially folded intermediate or even the formation of substantial amounts of intermolecular zinc-bridged AS species at the early stages of the aggregation process.

Although the results of this study begin to reveal the structural and molecular basis by which zinc accelerates AS amyloid fibril formation, more studies are needed to explore other biological aspects of AS–Zn^{2+} interactions. However, the low affinity that characterizes the interaction of Zn^{2+} with AS contrasts strongly with the high-affinity features reported for the binding of this metal ion to other target proteins linked to human amylodosis such as Aβ peptide and IAPP [58,91,98], challenging the biological relevance of zinc interactions in the pathogenesis of PD.

Acknowledgments

C.O.F. thanks ANPCyT, CONICET, Max Planck Society and the Alexander von Humboldt Foundation for financial support. C.O.F. is the head of a Partner Group of the Max Planck Institute for Biophysical Chemistry (Göttingen). A.A.V.G. is recipient of a fellowship from CONICET in Argentina. V.T.M. is recipient of a fellowship from ANPCyT in Argentina.

References

[1] C.M. Dobson, Semin. Cell Dev. Biol. 15 (2004) 3–16.
[2] F. Chiti, C.M. Dobson, Annu. Rev. Biochem. 75 (2006) 333–366.
[3] L.S. Forno, J. Neuropathol. Exp. Neurol. 55 (1996) 259–272.
[4] M. Goedert, Nat. Rev. Neurosci. 2 (2001) 492–501.
[5] M.G. Spillantini, M.L. Schmidt, V.M. Lee, J.Q. Trojanowski, R. Jakes, M. Goedert, Nature 388 (1997) 839–840.
[6] F.H. Lewy, Handbuch der Neurologie, Springer-Verlag, Berlin, Germany, 1912.
[7] J.M. George, Genome Biol. 3 (2002) 1–2.
[8] D. Eliezer, E. Kutluay, R. Bussell Jr., G. Browne, J. Mol. Biol. 307 (2001) 1061–1073.
[9] P.H. Weinreb, W. Zhen, A.W. Poon, K.A. Conway, P.T. Lansbury Jr., Biochemistry 35 (1996) 13709–13715.
[10] M.G. Spillantini, R.A. Crowther, R. Jakes, M. Hasegawa, M. Goedert, Proc. Natl. Acad. Sci. U. S. A. 95 (1998) 6469–6473.
[11] R. Kruger, W. Kuhn, T. Muller, D. Woitalla, M. Graeber, S. Kosel, H. Przuntek, J.T. Epplen, L. Schols, O. Riess, Nat. Genet. 18 (1998) 106–108.
[12] M.H. Polymeropoulos, C. Lavedan, E. Leroy, S.E. Ide, A. Dehejia, A. Dutra, B. Pike, H. Root, J. Rubenstein, R. Boyer, E.S. Stenroos, S. Chandrasekharappa, A. Athanassiadou, T. Papapetropoulos, W.G. Johnson, A.M. Lazzarini, R.C. Duvoisin, G. Di Iorio, L.I. Golbe, R.L. Nussbaum, Science 276 (1997) 2045–2047.
[13] J.J. Zarranz, J. Alegre, J.C. Gomez-Esteban, E. Lezcano, R. Ros, I. Ampuero, L. Vidal, J. Hoenicka, O. Rodriguez, B. Atares, V. Llorens, E. Gomez Tortosa, T. del Ser, D.G. Munoz, J.G. de Yebenes, Ann. Neurol. 55 (2004) 164–173.
[14] I. Martin, V.L. Dawson, T.M. Dawson, Annu. Rev. Genomics Hum. Genet. 12 (2011) 301–325.
[15] A.B. Singleton, M. Farrer, J. Johnson, A. Singleton, S. Hague, J. Kachergus, M. Hulihan, T. Peuralinna, A. Dutra, R. Nussbaum, S. Lincoln, A. Crawley, M. Hanson, D. Maraganore, C. Adler, M.R. Cookson, M. Muenter, M. Baptista, D. Miller, J. Blancato, J. Hardy, K. Gwinn-Hardy, Science 302 (2003) 841.
[16] M.B. Feany, W.W. Bender, Nature 404 (2000) 394–398.
[17] M. Hashimoto, E. Rockenstein, M. Mante, L. Crews, P. Bar-On, F.H. Gage, R. Marr, E. Masliah, Gene Ther. 11 (2004) 1713–1723.
[18] E. Masliah, E. Rockenstein, I. Veinbergs, M. Mallory, M. Hashimoto, A. Takeda, Y. Sagara, A. Sisk, L. Mucke, Science 287 (2000) 1265–1269.
[19] S. Hamamichi, R.N. Rivas, A.L. Knight, S. Cao, K.A. Caldwell, G.A. Caldwell, Proc. Natl. Acad. Sci. U. S. A. 105 (2008) 728–733.
[20] R. Bussell Jr., D. Eliezer, J. Mol. Biol. 329 (2003) 763–778.
[21] S. Chandra, X. Chen, J. Rizo, R. Jahn, T.C. Sudhof, J. Biol. Chem. 278 (2003) 15313–15318.
[22] C.C. Jao, A. Der-Sarkissian, J. Chen, R. Langen, Proc. Natl. Acad. Sci. U. S. A. 101 (2004) 8331–8336.
[23] B.I. Giasson, I.V. Murray, J.Q. Trojanowski, V.M. Lee, J. Biol. Chem. 276 (2001) 2380–2386.
[24] R.A. Crowther, R. Jakes, M.G. Spillantini, M. Goedert, FEBS Lett. 436 (1998) 309–312.
[25] C.O. Fernandez, W. Hoyer, M. Zweckstetter, E.A. Jares-Erijman, V. Subramaniam, C. Griesinger, T.M. Jovin, EMBO J. 23 (2004) 2039–2046.
[26] W. Hoyer, D. Cherny, V. Subramaniam, T.M. Jovin, Biochemistry 43 (2004) 16233–16242.
[27] C.W. Bertoncini, Y.S. Jung, C.O. Fernandez, W. Hoyer, C. Griesinger, T.M. Jovin, M. Zweckstetter, Proc. Natl. Acad. Sci. U. S. A. 102 (2005) 1430–1435.
[28] M.M. Dedmon, K. Lindorff-Larsen, J. Christodoulou, M. Vendruscolo, C.M. Dobson, J. Am. Chem. Soc. 127 (2005) 476–477.
[29] J.C. Lee, H.B. Gray, J.R. Winkler, J. Am. Chem. Soc. 127 (2005) 16388–16389.
[30] J.C. Lee, B.T. Lai, J.J. Kozak, H.B. Gray, J.R. Winkler, J. Phys. Chem. B 111 (2007) 2107–2112.
[31] E. Gaggelli, H. Kozlowski, D. Valensin, G. Valensin, Chem. Rev. 106 (2006) 1995–2044.

[32] H. Kozlowski, D.R. Brown, G. Valensin, Metallochemistry of Neurodegeneration: Biological, Chemical and Genetic Aspects, Royal Society of Chemistry, Cambridge, 2006.
[33] D.R. Brown, F. Hafiz, L.L. Glasssmith, B.S. Wong, I.M. Jones, C. Clive, S.J. Haswell, EMBO J. 19 (2000) 1180–1186.
[34] D.R. Brown, H. Kozlowski, Dalton Trans. (2004) 1907–1917.
[35] E. Gaggelli, F. Bernardi, E. Molteni, R. Pogni, D. Valensin, G. Valensin, M. Remelli, M. Luczkowski, H. Kozlowski, J. Am. Chem. Soc. 127 (2005) 996–1006.
[36] M. Klewpatinond, P. Davies, S. Bowen, D.R. Brown, J.H. Viles, J. Biol. Chem. 283 (2008) 1870–1881.
[37] D.R. Brown, Dalton Trans. (2009) 4069–4076.
[38] J.W. Karr, V.A. Szalai, Biochemistry 47 (2008) 5006–5016.
[39] N.H. Kim, J.K. Choi, B.H. Jeong, J.I. Kim, M.S. Kwon, R.I. Carp, Y.S. Kim, FASEB J. 19 (2005) 783–785.
[40] P. Faller, C. Hureau, Dalton Trans. (2009) 1080–1094.
[41] S.C. Drew, C.L. Masters, K.J. Barnham, J. Am. Chem. Soc. 131 (2009) 8760–8761.
[42] S.C. Drew, C.J. Noble, C.L. Masters, G.R. Hanson, K.J. Barnham, J. Am. Chem. Soc. 131 (2009) 1195–1207.
[43] M. Klewpatinond, J.H. Viles, Biochem. J. 404 (2007) 393–402.
[44] T. Kowalik-Jankowska, M. Ruta, K. Wisniewska, L. Lankiewicz, J. Inorg. Biochem. 95 (2003) 270–282.
[45] C.D. Syme, R.C. Nadal, S.E. Rigby, J.H. Viles, J. Biol. Chem. 279 (2004) 18169–18177.
[46] D. Valensin, M. Luczkowski, F.M. Mancini, A. Legowska, E. Gaggelli, G. Valensin, K. Rolka, H. Kozlowski, Dalton Trans. (2004) 1284–1293.
[47] D. Valensin, F.M. Mancini, M. Luczkowski, A. Janicka, K. Wisniewska, E. Gaggelli, G. Valensin, L. Lankiewicz, H. Kozlowski, Dalton Trans. (2004) 16–22.
[48] J.H. Viles, F.E. Cohen, S.B. Prusiner, D.B. Goodin, P.E. Wright, H.J. Dyson, Proc. Natl. Acad. Sci. U. S. A. 96 (1999) 2042–2047.
[49] P. Dorlet, S. Gambarelli, P. Faller, C. Hureau, Angew. Chem. Int. Ed Engl. 48 (2009) 9273–9276.
[50] H. Eury, C. Bijani, P. Faller, C. Hureau, Angew. Chem. Int. Ed Engl. 50 (2011) 901–905.
[51] C. Hureau, V. Balland, Y. Coppel, P.L. Solari, E. Fonda, P. Faller, J. Biol. Inorg. Chem. 14 (2009) 995–1000.
[52] E. Aronoff-Spencer, C.S. Burns, N.I. Avdievich, G.J. Gerfen, J. Peisach, W.E. Antholine, H.L. Ball, F.E. Cohen, S.B. Prusiner, G.L. Millhauser, Biochemistry 39 (2000) 13760–13771.
[53] B. Belosi, E. Gaggelli, R. Guerrini, H. Kozlowski, M. Luczkowski, F.M. Mancini, M. Remelli, D. Valensin, G. Valensin, Chembiochem 5 (2004) 349–359.
[54] C.S. Burns, E. Aronoff-Spencer, C.M. Dunham, P. Lario, N.I. Avdievich, W.E. Antholine, M.M. Olmstead, A. Vrielink, G.J. Gerfen, J. Peisach, W.G. Scott, G.L. Millhauser, Biochemistry 41 (2002) 3991–4001.
[55] M. Chattopadhyay, E.D. Walter, D.J. Newell, P.J. Jackson, E. Aronoff-Spencer, J. Peisach, G.J. Gerfen, B. Bennett, W.E. Antholine, G.L. Millhauser, J. Am. Chem. Soc. 127 (2005) 12647–12656.
[56] C.E. Jones, S.R. Abdelraheim, D.R. Brown, J.H. Viles, J. Biol. Chem. 279 (2004) 32018–32027.
[57] H. Kozlowski, M. Luczkowski, M. Remelli, D. Valensin, Coord. Chem. Rev. (2012), http://dx.doi.org/10.1016/j.ccr.2012.03.013.
[58] J. Danielsson, R. Pierattelli, L. Banci, A. Graslund, FEBS J. 274 (2007) 46–59.
[59] Y. Mekmouche, Y. Coppel, K. Hochgrafe, L. Guilloreau, C. Talmard, H. Mazarguil, P. Faller, Chembiochem 6 (2005) 1663–1671.
[60] N. Rezaei-Ghaleh, K. Giller, S. Becker, M. Zweckstetter, Biophys. J. 101 (2011) 1202–1211.
[61] C.D. Syme, J.H. Viles, Biochim. Biophys. Acta 1764 (2006) 246–256.
[62] D.T. Dexter, A. Carayon, F. Javoy-Agid, Y. Agid, F.R. Wells, S.E. Daniel, A.J. Lees, P. Jenner, C.D. Marsden, Brain 114 (1991) 1953–1975.
[63] R.J. Castellani, S.L. Siedlak, G. Perry, M.A. Smith, Acta Neuropathol. 100 (2000) 111–114.
[64] H.S. Pall, D.R. Blake, J.M. Gutteridge, A.C. Williams, J. Lunec, M. Hall, A. Taylor, Lancet 330 (1987) 238–241.
[65] P. Riederer, E. Sofic, W.D. Rausch, B. Schmidt, G.P. Reynolds, K. Jellinger, M.B. Youdim, J. Neurochem. 52 (1989) 515–520.
[66] D.T. Dexter, F.R. Wells, A.J. Lees, F. Agid, Y. Agid, P. Jenner, C.D. Marsden, J. Neurochem. 52 (1989) 1830–1836.
[67] L. Breydo, J.W. Wu, V.N. Uversky, Biochim. Biophys. Acta 1822 (2012) 261–285.
[68] L. Breydo, V.N. Uversky, Metallomics 3 (2011) 1163–1180.
[69] J.M. Gorell, C.C. Johnson, B.A. Rybicki, E.L. Peterson, G.X. Kortsha, G.G. Brown, R.J. Richardson, Neurotoxicology 20 (1999) 239–247.
[70] R.M. Rasia, C.W. Bertoncini, D. Marsh, W. Hoyer, D. Cherny, M. Zweckstetter, C. Griesinger, T. Jovin, C.O. Fernández, Proc. Natl. Acad. Sci. U. S. A. 102 (2005) 4294–4299.
[71] A. Binolfi, R.M. Rasia, C.W. Bertoncini, M. Ceolin, M. Zweckstetter, C. Griesinger, T.M. Jovin, C.O. Fernandez, J. Am. Chem. Soc. 128 (2006) 9893–9901.
[72] M.J. Hokenson, V.N. Uversky, J. Goers, G. Yamin, L.A. Munishkina, A.L. Fink, Biochemistry 43 (2004) 4621–4633.
[73] C. Andre, T.T. Truong, J.F. Robert, Y.C. Guillaume, Electrophoresis 26 (2005) 3256–3264.
[74] T.D. Kim, S.R. Paik, C.H. Yang, J. Kim, Protein Sci. 9 (2000) 2489–2496.
[75] G. Yamin, C.B. Glaser, V.N. Uversky, A.L. Fink, J. Biol. Chem. 278 (2003) 27630–27635.
[76] Y. Fezoui, D.M. Hartley, J.D. Harper, R. Khurana, D.M. Walsh, M.M. Condron, D.J. Selkoe, P.T. Lansbury Jr., A.L. Fink, D.B. Teplow, Amyloid 7 (2000) 166–178.
[77] M. Rückert, G. Otting, J. Am. Chem. Soc. 122 (2000) 7793–7797.
[78] F. Delaglio, S. Grzesiek, G.W. Vuister, G. Zhu, J. Pfeifer, A. Bax, J. Biomol. NMR 6 (1995) 277–293.
[79] J. Cavanagh, W.J. Fairbrother, A.G.I. Palmer, M. Rance, N.J. Skelton, Protein NMR Spectroscopy: Principles and Practice, Second Edition Elsevier Academic Press, California, U.S.A., 2007.
[80] A. Binolfi, G.R. Lamberto, R. Duran, L. Quintanar, C.W. Bertoncini, J.M. Souza, C. Cervenansky, M. Zweckstetter, C. Griesinger, C.O. Fernandez, J. Am. Chem. Soc. 130 (2008) 11801–11812.
[81] A. Binolfi, E.E. Rodriguez, D. Valensin, N. D'Amelio, E. Ippoliti, G. Obal, R. Duran, A. Magistrato, O. Pritsch, M. Zweckstetter, G. Valensin, P. Carloni, L. Quintanar, C. Griesinger, C.O. Fernandez, Inorg. Chem. 49 (2010) 10668–10679.
[82] G.R. Lamberto, A. Binolfi, M.L. Orcellet, C.W. Bertoncini, M. Zweckstetter, C. Griesinger, C.O. Fernandez, Proc. Natl. Acad. Sci. U. S. A. 106 (2009) 21057–21062.
[83] G.R. Lamberto, V. Torres-Monserrat, C.W. Bertoncini, X. Salvatella, M. Zweckstetter, C. Griesinger, C.O. Fernandez, J. Biol. Chem. 286 (2011) 32036–32044.
[84] P. Kuzmic, Anal. Biochem. 237 (1996) 260–273.
[85] C.J. Frederickson, J.Y. Koh, A.I. Bush, Nat. Rev. Neurosci. 6 (2005) 449–462.
[86] R.A. Cherny, J.T. Legg, C.A. McLean, D.P. Fairlie, X. Huang, C.S. Atwood, K. Beyreuther, R.E. Tanzi, C.L. Masters, A.I. Bush, J. Biol. Chem. 274 (1999) 23223–23228.
[87] P. Bernado, C.W. Bertoncini, C. Griesinger, M. Zweckstetter, M. Blackledge, J. Am. Chem. Soc. 127 (2005) 17968–17969.
[88] H. Sigel, R.B. Martin, Chem. Rev. 82 (1982) 385–426.
[89] I. Sovago, K. Osz, Dalton Trans. (2006) 3841–3854.
[90] R.J. Sundberg, R.B. Martin, Chem. Rev. 74 (1974) 471–517.
[91] D. Valensin, F. Camponeschi, M. Luczkowski, M.C. Baratto, M. Remelli, G. Valensin, H. Kozlowski, Metallomics 3 (2011) 292–302.
[92] S. Salamekh, J.R. Brender, S.J. Hyung, R.P. Nanga, S. Vivekanandan, B.T. Ruotolo, A. Ramamoorthy, J. Mol. Biol. 410 (2011) 294–306.
[93] P. Faller, Chembiochem 10 (2009) 2837–2845.
[94] N.G. Nair, G. Perry, M.A. Smith, V.P. Reddy, J. Alzheimers Dis. 20 (2010) 57–66.
[95] R. Aruga, Transit. Met. Chem. 8 (1983) 56–58 Springer Netherlands.
[96] A. Chakravorty, F.A. Cotton, J. Phys. Chem. 67 (1963) 2878–2879.
[97] A. Clements, D. Allsop, D.M. Walsh, C.H. Williams, J. Neurochem. 66 (1996) 740–747.
[98] C. Talmard, A. Bouzan, P. Faller, Biochemistry 46 (2007) 13658–13666.
[99] J.R. Brender, K. Hartman, R.P. Nanga, N. Popovych, R. de la Salud Bea, S. Vivekanandan, E.N. Marsh, A. Ramamoorthy, J. Am. Chem. Soc. 132 (2010) 8973–8983.
[100] V. Minicozzi, F. Stellato, M. Comai, M. Dalla Serra, C. Potrich, W. Meyer-Klaucke, S. Morante, J. Biol. Chem. 283 (2008) 10784–10792.
[101] Y. Miller, B. Ma, R. Nussinov, Proc. Natl. Acad. Sci. U. S. A. 107 (2010) 9490–9495.
[102] D.S. Auld, Biometals 22 (2009) 141–148.
[103] B.L. Vallee, D.S. Auld, Biochemistry 29 (1990) 5647–5659.
[104] D. Noy, I. Solomonov, O. Sinkevich, T. Arad, K. Kjaer, I. Sagi, J. Am. Chem. Soc. 130 (2008) 1376–1383.
[105] I. Solomonov, E. Korkotian, B. Born, Y. Feldman, A. Bitler, F. Rahimi, H. Li, G. Bitan, I. Sagi, J. Biol. Chem. 287 (2012) 20555–20564.
[106] V.N. Uversky, J. Li, A.L. Fink, J. Biol. Chem. 276 (2001) 10737–10744.
[107] V.N. Uversky, J. Li, A.L. Fink, J. Biol. Chem. 276 (2001) 44284–44296.